

# PCCP

Accepted Manuscript



This is an *Accepted Manuscript*, which has been through the Royal Society of Chemistry peer review process and has been accepted for publication.

*Accepted Manuscripts* are published online shortly after acceptance, before technical editing, formatting and proof reading. Using this free service, authors can make their results available to the community, in citable form, before we publish the edited article. We will replace this *Accepted Manuscript* with the edited and formatted *Advance Article* as soon as it is available.

You can find more information about *Accepted Manuscripts* in the [Information for Authors](#).

Please note that technical editing may introduce minor changes to the text and/or graphics, which may alter content. The journal's standard [Terms & Conditions](#) and the [Ethical guidelines](#) still apply. In no event shall the Royal Society of Chemistry be held responsible for any errors or omissions in this *Accepted Manuscript* or any consequences arising from the use of any information it contains.

# The Binding and Insertion of Imidazolium-based Ionic Surfactants into Lipid Bilayers: the Effects of Surfactant Size and Salt Concentration

Hwankyu Lee<sup>1,\*</sup>, Tae-Joon Jeon<sup>2</sup>

<sup>1</sup>Department of Chemical Engineering, Dankook University, Yongin, 448-701, South Korea

<sup>2</sup>Department of Biological Engineering, Inha University, Incheon, 402-751, South Korea

\*Corresponding author

Email: [leeh@dankook.ac.kr](mailto:leeh@dankook.ac.kr)

**Abstract**

Imidazolium-based ionic surfactants with hydrocarbon tails of different sizes were simulated with lipid bilayers at different salt concentrations. Starting with the random position of ionic surfactants outside the bilayer, surfactants with long tails mostly insert into the bilayer, while those with short tails show the insertion of fewer surfactant molecules, indicating the effect of the tail length. In particular, surfactants with the tail of two or four hydrocarbons insert and reversibly detach from the bilayer, while the inserted longer surfactants cannot be reversibly detached because of the strong hydrophobic interaction with lipid tails, in quantitative agreement with experiments. Longer surfactants more deeply and irreversibly insert into the bilayer and thus increase lateral diffusivities of the bilayer, indicating that longer surfactants more significantly disorder lipid bilayers, which also agrees with experiments regarding the effect of the tail length of ionic surfactants on membrane permeability and toxicity. Addition of NaCl ions weakens the electrostatic interactions between head groups of surfactants and lipids, leading to the binding of fewer surfactants into the bilayer. In particular, our simulation findings indicate that insertion of ionic surfactants can be initiated by either the hydrophobic interaction between tails of surfactants and lipids or the electrostatic binding between imidazolium heads and lipid heads, and the strength of hydrophobic and electrostatic interactions depends on the tail length of surfactants.

## Introduction

Ionic liquids (ILs) are organic or inorganic salts in liquid phase at room temperature. Because ILs have low volatility, non-combustibility, and high thermal and chemical stability,<sup>1-4</sup> they have shown great potential for use as electrolytes or sorption media for many chemical or biological applications such as battery,<sup>5, 6</sup> separation process,<sup>7, 8</sup> catalysis,<sup>9, 10</sup> and cellulose processing.<sup>11</sup> Although ILs have been widely used as safe electrolytes for many industrial applications,<sup>12, 13</sup> experiments at the organism level have shown that ILs are toxic to biological organisms in aquatic environment,<sup>14-19</sup> indicating that their industrial applications should be reconsidered with caution. To develop ILs with low toxicity while still maintaining high efficiency, the dependence of toxicity on the conformation and structure of ILs needs to be understood, which has motivated experimental studies at the higher resolution.

Evans pioneered the experimental studies of the interactions between imidazolium-based ionic surfactants and membranes,<sup>20-22</sup> showing that the instability and permeability of liposomes or supported lipid bilayers increase as the tail length of surfactants increases, which indicates that membranes are disordered mainly by the hydrophobic interactions between surfactants and lipid tails. Recently, Jeong et al. showed that ionic surfactants with longer hydrocarbon tails at higher concentrations induce the lower transition temperature of liposomes,<sup>23</sup> again indicating the effect of the surfactant-tail length. Also, Galluzzi et al. electrochemically characterized the interactions between ionic surfactants and phospholipid monolayers, showing that the strength of the surfactant-monolayer interaction is controlled by the length of hydrocarbon tails rather than by the charge interactions between surfactants and lipid headgroups.<sup>24</sup> In particular, they found that ionic surfactants with short tails adsorb onto the monolayer and then detach from it, showing the reversible interaction, while those with longer tails insert into the bilayer but cannot reversibly

detach from it. Rapid cyclic voltammetry experiments showed the higher extent of toxicity for ionic surfactants with longer tails. They suggested that when ionic surfactants penetrate into the bilayer, surfactant tails may first migrate toward the tail region of the membrane, although the mechanism of the binding and insertion of surfactants into membranes has not been experimentally well studied because of the limited resolution.

To support and complement experimental observations, molecular dynamics (MD) simulations have been performed to understand the interactions between imidazolium-based ionic surfactants and bilayers. Ballone and coworkers simulated ionic surfactants with butyl tails in cholesterol bilayers, showing that surfactants adsorb into the bilayer, while counterions mostly dissolved in water and only partially interact with the bilayer surface.<sup>25</sup> They also simulated those surfactants in phospholipid bilayers, showing that when surfactants penetrate into the bilayer, surfactant tails first insert into the bilayer, which influences membrane properties.<sup>26</sup> Recently, Klahn and Zacharias simulated ionic surfactants with longer tails in model membranes with different ratios of cholesterol and anionic phospholipids, and their free energy calculations showed that cholesterol modulate the structural and electrostatic properties of membranes and thus inhibit the ionic-surfactant insertion.<sup>27</sup> These simulations indicate that ionic surfactants insert into lipid bilayers due to the hydrophobic interaction between tails of surfactants and lipids, but the binding and insertion dependence on the ionic-surfactant tail length and the salt concentration has not been systematically studied through computation.

As a further step toward understanding the binding and insertion of ionic surfactants into membranes, here we report MD simulations of imidazolium-based ionic surfactants with hydrocarbon tails of four different lengths in phospholipid bilayers at 0 and 0.5 M NaCl. To understand the effect of the surfactant-tail length, the extents of random adsorption of surfactants

and membrane disruption are analyzed by quantifying the numbers and positions of the inserted surfactants, density profiles, and lateral diffusivities of lipids, which support the experimental observations of the reversible interactions between short ionic surfactants and bilayers. Also, the strength of the surfactant-bilayer interaction is analyzed at different salt concentrations. Finally, the dependence of the binding and insertion on the surfactant length and salt concentration is rationalized by considering their electrostatic and hydrophobic interactions with lipid head and tail groups.

## Methods

All simulations and analyses were performed using the GROMACS4.5.5 simulation package<sup>28-30</sup> with the OPLS all-atom force field (FF) and TIP4P water model.<sup>31, 32</sup> Potential parameters for dioleoylglycerophosphocholine (DOPC) lipids were taken from the Berger lipid FF modified by Tieleman et al., which can be compatibly used with the OPLS FF and predict the experimentally observed areas per lipid and dynamics of DOPC bilayers.<sup>33, 34</sup> For imidazolium-based ionic surfactants, Sambasivarao and Acevedo parameterized the OPLS ionic-liquid FF, which has successfully captured the structural and thermodynamic properties of ionic surfactants and their solvent effects on the conformation of polymer chains, in agreement with experiments and polymer theories.<sup>35, 36</sup> Thus, this OPLS ionic-liquid FF has been widely used for many other simulations,<sup>37-40</sup> and here we use this FF to model four ionic surfactants, 1-ethyl-3-methylimidazolium (C<sub>2</sub>MIM), 1-butyl-3-methylimidazolium (C<sub>4</sub>MIM), 1-hexyl-3-methylimidazolium (C<sub>6</sub>MIM), and 1-decyl-3-methylimidazolium (C<sub>10</sub>MIM), where this FF distinguishes partial charges and dihedral potentials for EMIM, BMIM, and other longer ones.

16 or 60 ionic surfactants were randomly added to the water region of the equilibrated

bilayer system (Figure 1, left). Since each surfactant has a net charge of +1, 16 or 60 counterions (Cl<sup>-</sup>) were added to neutralize the systems. Also, 79 NaCl ions were additionally added to generate the ion concentration of 0.5 M, as shown in Table 1. The final simulated system consists of 16 (or 60) ionic surfactant, 128 DOPC (64 DOPC/leaflet), ~8,000 TIP4P water, and 16-95 ion (Na<sup>+</sup> and Cl<sup>-</sup>) molecules in a periodic box of size  $7 \times 7 \times 9$  nm<sup>3</sup>. Real space cutoffs of 14 Å and 11 Å were respectively applied for Lennard-Jones and electrostatic forces with the inclusion of particle mesh Ewald summation for long-range electrostatics.<sup>41</sup> A temperature of 298 K and a pressure of 1 bar were maintained by applying the velocity-rescale thermostat<sup>42</sup> and Berendsen barostat<sup>43</sup> in the NP<sub>xy</sub>P<sub>z</sub>T ensemble (semi-isotropic pressure coupling). The LINCS algorithm was used to constrain the bond lengths.<sup>44</sup> Simulations were performed for 250 ns with a time step of 2 fs on computational facilities supported by the National Institute of Supercomputing and Networking/Korea Institute of Science and Technology Information with supercomputing resources including technical support (KSC-2014-C3-068). The last-30 ns trajectories were used for analyses.

## Results and Discussion

Imidazolium-based ionic surfactants with hydrocarbon tails of four different lengths were simulated at different concentrations of surfactants and NaCl for 250 ns. Simulated systems are named in Table 1. “C<sub>*n*</sub>M” indicates the imidazolium surfactants, where *n* is the number of hydrocarbons per surfactant tail. The number, “16” or “60”, describes the number of surfactant molecules in the system, which are followed by “i” for the system at 0.5 M NaCl. For example, “C<sub>10</sub>M60” designates a bilayer with 60 C<sub>10</sub>MIM molecules with counterions, while “C<sub>6</sub>M16i” indicates that the bilayer system includes 16 C<sub>6</sub>MIM molecules with counterions and additional

ions of 0.5 M NaCl.

### **Binding and insertion dependence on the ionic-surfactant length and salt concentration**

Figure 1 shows snapshots from the beginning (left) and end of simulations (columns 2-7). Ionic surfactants, which were initially randomly distributed in the solvent region, insert into lipid bilayers, but their insertion extents differ. Most surfactants insert into the lipid bilayer in C<sub>4</sub>M16, C<sub>6</sub>M16, and C<sub>10</sub>M16, while C<sub>2</sub>M16 shows the insertion of much fewer surfactants, indicating the effect of the tail length. For ionic surfactants with tails of the same size, fewer surfactants insert into the bilayer at 0.5 M NaCl than at 0 M, implying that NaCl ions may inhibit the insertion of surfactants into the bilayer. For the systems with C<sub>2</sub>MIM and C<sub>10</sub>MIM, ionic surfactants of higher concentrations were also simulated, showing insertion of surfactants as well as the micelle formation.

To quantify the extent of insertion, the numbers of the inserted surfactants were calculated as a function of time. Figure 2 shows that for the systems with 16 surfactants, only ~5 C<sub>2</sub>MIMs insert into the bilayer, while surfactants with longer tails mostly insert into lipid bilayers, indicating more insertion of surfactants with longer tails, as observed in Galluzzi et al.'s experiments.<sup>24</sup> In particular, the numbers of the inserted C<sub>2</sub>MIMs and C<sub>4</sub>MIMs significantly fluctuate, while the numbers of the inserted C<sub>6</sub>MIM and C<sub>10</sub>MIM linearly increase without much fluctuation. This implies that ionic surfactants with short tails may reversibly insert and detach from the bilayer, while those with longer tails irreversibly bind to the bilayer, which will be discussed in the following section. Since longer surfactants show more insertion and irreversible interaction with the bilayer, longer tails of surfactants may have the stronger hydrophobic interactions with lipid tails. To resolve this, we calculated the average number of carbon atoms of

DOPC tails close to the surfactant tail, and the cumulative number of those as a function of distance from the surfactant tail. Here, if the distance between hydrocarbon tails of surfactants and DOPC lipids is less than 0.6 nm, they are considered to be close. In Figure 3, the numbers of DOPC-tail carbons close to surfactant tails increase as a function of time, showing the order  $C_{10}M16 > C_6M16 > C_4M16 > C_2M16$ . This tendency is confirmed in their cumulative numbers as a function of distance from the surfactant tail, indicating that ionic surfactants with longer tails have the stronger hydrophobic interaction with DOPC tails and thus induce insertion of more surfactant molecules. Cumulative numbers also show that other criteria with the distance from 0.5 to 1 nm produce similar qualitative trends, conforming that the analysis does not significantly depend on the distance criteria. In Figure 2, for the systems with the same-sized surfactants at different salt concentrations, fewer surfactants are inserted at 0.5 M NaCl than at 0 M NaCl, presumably because NaCl ions weaken the electrostatic interactions between cationic surfactant headgroups and anionic lipid phosphates, leading to the less binding. These indicate that insertion of ionic surfactants is controlled not by any single factor, but by a combination of the hydrophobic interaction with lipid tails and the electrostatic interaction with lipid heads. For the systems with 60 surfactants, more surfactants insert into the bilayer than do those for the systems with 16 surfactants, showing more insertion at higher concentrations. Note that the number of inserted surfactants drastically increases as the surfactant-tail length increases, showing the order  $C_6M60 > C_4M60 > C_2M60$ , while this concentration effect does not even occur in  $C_{10}M60$ , presumably because long surfactants ( $C_{10}MIM$ ) tend to form micelles at the high concentration, as visualized in Figure 1. These indicate more insertion of ionic surfactants at higher concentrations, but this concentration effect depends on the length of surfactant tails.

These configurations and the insertion extent of ionic surfactants are also confirmed by

calculating density profiles. Figure 4 shows that there are fewer surfactants inside the bilayer for the systems with shorter surfactants and more NaCl ions, consistent with Figures 1 and 2. Since C<sub>2</sub>MIM and C<sub>4</sub>MIM have short hydrocarbon tails, surfactant tails are not observed inside the bilayer. However, the systems with C<sub>6</sub>MIM and C<sub>10</sub>MIM clearly show that surfactant tails are in the hydrophobic-tail region of the bilayer, again confirming the strong hydrophobic interaction between tails of surfactants and lipids, consistent with Figure 3. Figure 4 also shows that cationic imidazolium heads interact with anionic DOPC phosphates, implying that their charge interactions may influence the binding of surfactants into the bilayer. For the systems with 60 surfactants, many surfactants are observed outside the bilayer, showing that densities of the inserted surfactants are almost same as those for the systems with 16 surfactants. Na and Cl ions are broadly positioned in the system, although they are slightly more concentrated on the bilayer surface. Note that previous simulations of lipid bilayers with NaCl have shown that Na ions strongly interact with lipid phosphates, while Cl ions mostly interact with water.<sup>45</sup> In Figure 4, Na ions are concentrated around anionic DOPC phosphates, which can reduce the electrostatic binding of cationic imidazolium heads of surfactants into the bilayer surface, leading to the less insertion of surfactants as shown in Figure 2. In Figure 5, radial distribution functions between DOPC phosphates and Na ions show high peaks for surfactants of all lengths, indicating the strong phosphate-Na interactions. RDF peaks for C<sub>6</sub>M16i and C<sub>10</sub>M16i are lower than those for C<sub>2</sub>M16i and C<sub>4</sub>M16i, as expected, since cationic ionic surfactants with longer tails are more inserted, which can weaken the charge interaction between Na and DOPC phosphates. These results indicate that NaCl ions weaken the electrostatic interactions between ionic surfactants and lipid headgroups, leading to the binding and insertion of fewer surfactants.

### Reversibility of the ionic surfactant-bilayer interaction and bilayer disorder

As discussed above, ionic surfactants with short tails may reversibly insert into the bilayer and detach from it, while those with long tails cannot reversibly interact with the bilayer. To examine this, the insertion of surfactants into the bilayer was further quantified by calculating the coordinate of the terminal carbon of each surfactant's tail in the bilayer normal direction ( $z$ -direction). Figure 6 shows that C<sub>2</sub>MIM molecules repeatedly insert into the bilayer and then detach from it for whole simulation time, indicating the reversible interaction between surfactants and the bilayer. C<sub>4</sub>MIM molecules also show the same trend, although reversible interactions are less observed than for the system with C<sub>2</sub>MIM. In contrast, once C<sub>6</sub>MIM and C<sub>10</sub>MIM molecules insert into the bilayer, they do not detach from the bilayer for whole simulation time. This indicates that C<sub>2</sub>MIM and C<sub>4</sub>MIM reversibly interact with lipid bilayers, while C<sub>6</sub>MIM and C<sub>10</sub>MIM do not, which quantitatively agrees with Galluzzi et al.'s experiments that showed that C<sub>2</sub>MIM and C<sub>4</sub>MIM have the reversible interaction with DOPC monolayers, while C<sub>8</sub>MIM and C<sub>12</sub>MIM have the irreversible interaction.<sup>24</sup> In Figure 6, terminal carbons are more deeply inserted as the tail length of surfactant increases, indicating the deeper insertion of longer surfactants because of the stronger hydrophobic interaction.

These results imply that longer ionic surfactants adsorb more deeply into the bilayer and thus may more effectively disorder lipid bilayers. This was also observed in experiments, showing that longer surfactants more significantly decrease the liposome stability and increase monolayer permeability and cytotoxicity.<sup>23,24</sup> To investigate this, lateral diffusion coefficients of DOPC lipids were calculated from the slopes of the mean-square displacements (MSDs) in the  $xy$ -plane (the direction perpendicular to the bilayer normal). Note that for the calculation of MSD from MD simulations of cubic boxes with periodic boundary conditions, the MSD needs to

be corrected for finite size effects using Yeh and Hummer's analytic formula.<sup>46</sup> For bilayers in noncubic boxes, the analytic equation is not clearly formulated. Also, the size effect should not significantly affect the comparison of lateral diffusivities because the sizes of simulated systems do not differ. Thus, the finite size effect is not corrected here. We calculated the lateral diffusion coefficient of pure DOPC bilayer, showing that the diffusivity is  $0.74 (\pm 0.15) \times 10^{-7} \text{ cm}^2 \text{ s}^{-1}$  at 298 K, close to the experimental value of  $0.82 \times 10^{-7} \text{ cm}^2 \text{ s}^{-1}$ ,<sup>47</sup> indicating that lateral diffusivities can be accurately predicted by simulations. Figure 7 shows that the addition of ionic surfactants increases lateral diffusivities, indicating that surfactants disorder lipid bilayers, although the increased extents differ. For C<sub>2</sub>M16, C<sub>4</sub>M16, and C<sub>6</sub>M16, lateral diffusivities are only slightly higher than for the pure DOPC bilayer, while the diffusivity drastically increases for C<sub>10</sub>M16. In particular, the numbers of the inserted surfactants are same for the systems C<sub>4</sub>M16, C<sub>6</sub>M16, and C<sub>10</sub>M16, but lateral diffusivities for C<sub>10</sub>M16 are much higher than those for others. These indicate that longer ionic surfactants more significantly disorder lipid bilayers, even when the same amount of surfactant molecules insert. Note that although much more surfactant molecules insert in C<sub>4</sub>M16 and C<sub>6</sub>M16 than in C<sub>2</sub>M16, their lateral diffusivities are almost same, indicating that short surfactants cannot disorder lipids even at the high surfactant concentration in the bilayer. These results imply that the longer ionic-surfactant tails more significantly destabilize lipid bilayers and thus can increase membrane permeability and toxicity, as observed in experiments.<sup>23,24</sup>

### **Micelle formation at the high concentration of surfactant**

Figure 2 shows that, although C<sub>10</sub>M60 has almost four times as many C<sub>10</sub>MIM molecules as does C<sub>10</sub>M16, the numbers of the inserted C<sub>10</sub>MIM do not significantly differ,

indicating that the higher concentration of surfactants does not increase the extent of insertion, presumably because of the micelle formation of ionic surfactants, as visualized in Figure 1. To understand the formation of micelles, the numbers of surfactants in the largest surfactant cluster were calculated for all simulated systems. Here, if the distance between terminal groups of different surfactant tails is less than 0.6 nm, then those surfactants are considered to be a cluster. Other criteria with the distance from 0.6 to 0.9 nm produce similar qualitative trends, as also observed in our previous work.<sup>48-50</sup> In Figure 8, C<sub>10</sub>M16 shows no cluster formation, since most surfactants insert into the bilayer. However, C<sub>10</sub>M60 shows the formation of the cluster composed of ~14 surfactant molecules, as visualized in Figure 8. These surfactant aggregation and micelle formation occur in C<sub>10</sub>M60, but not in C<sub>2</sub>M60, C<sub>4</sub>M60, and C<sub>6</sub>M60, indicating that tail lengths of C<sub>2</sub>MIM, C<sub>4</sub>MIM, and C<sub>6</sub>MIM are too short to induce the strong hydrophobic interaction for the micelle formation even at the high concentration, although it cannot be ruled out that the micelle formation might eventually occur in the system with more than 60 surfactants. For C<sub>10</sub>M16i, ~5 free surfactants form the cluster, showing an incomplete micelle, again indicating the tendency for the micelle formation of surfactants with long tails. It would obviously be interesting to further simulate micelles of ionic surfactants to understand its dependence on the ionic-surfactant and salt concentrations, which would be computationally very expensive and thus beyond the scope of this paper. Whether or not the results here can explain the micelle formation of ionic surfactants, simulations show that the higher concentration of surfactants does not necessarily lead to more insertion because they can induce the higher extent of aggregation and micelle formation.

### **Electrostatic and hydrophobic interactions between ionic surfactants and lipids**

Since ionic surfactants with longer tails have the stronger hydrophobic interaction with lipid tails and irreversibly interact with lipid bilayers, the surfactant-bilayer interaction seems to depend only on the hydrophobicity, but the charge interactions between surfactants and lipids may be also important. Note that tails of C<sub>2</sub>MIM and C<sub>4</sub>MIM are too short to induce the strong hydrophobic interaction with lipid tails, showing the reversible interaction with bilayers, and hence their binding and insertion may be influenced by the charge interaction. To understand this, the effects of electrostatic and hydrophobic interactions on the surfactant binding and insertion were investigated.

Figure 9 visualizes two cases for the insertion of surfactants into the bilayer. In Figure 9 (top), the surfactant headgroup first binds to the lipid headgroup apparently because of their charge interactions, and then the surfactant tail inserts into the bilayer due to the hydrophobic interaction. For the other case (Figure 9, bottom), the surfactant tail binds to the bilayer surface and slides through the bilayer interior, showing the binding and insertion dependence only on the hydrophobic interaction. These indicate that the binding and insertion of surfactants into the bilayer are attributed to both electrostatic and hydrophobic interactions, although the insertion of surfactants is mainly due to the hydrophobic interaction. To understand the strength of electrostatic and hydrophobic interactions, we calculated radial distribution functions (RDFs) between the phosphorus atoms of DOPC and the center of mass (COM) of the surfactant headgroup, and RDFs between the tail groups of DOPC and the terminal carbons of surfactants. In Figure 10, both hydrophobic and electrostatic interactions show lower peaks for C<sub>2</sub>M16 than for other surfactants with longer tails. This is expected, since much fewer surfactants insert in C<sub>2</sub>M16 than in other systems. However, the RDF height for surfactant-lipid headgroups of C<sub>2</sub>M16 is approximately a half of those for other systems, while the RDF height for surfactant-

lipid tails is much lower for C<sub>2</sub>M16 than for others, indicating that as the surfactant-tail length decreases, their hydrophobic interactions with lipid tails become significantly weaker, which implies that the binding and insertion of surfactants with short tails mostly depend on the electrostatic interaction.

These results, combined with the observations in Figures 2-6, indicate that ionic surfactants with short tails bind and insert into lipid bilayers mainly because of the electrostatic interaction, where their tails are not long enough to form the strong hydrophobic interaction, leading to the reversible binding and insertion of surfactants into the bilayer, in agreement with experiments.<sup>24</sup> For ionic surfactants with longer tails, surfactants have the stronger hydrophobic interactions with lipid tails, leading to the deeper insertion of more surfactants, the irreversible interactions with the bilayer, and the increased lateral dynamics of the bilayer, which support the experimental observations that showed that membrane permeability and toxicity depend on the length of the ionic-surfactant tail.

## Conclusions

We performed MD simulations of imidazolium-based ionic surfactants with tails of 2, 4, 6, and 10 hydrocarbons in DOPC bilayers at the salt concentrations of 0 and 0.5 M NaCl. Ionic surfactants, which were initially randomly distributed in the solvent region outside the bilayer, insert into the bilayer, where the insertion extent depends on the tail length. For surfactants with long tails, most surfactants insert into the bilayer and then cannot reversibly detach from it because of their strong hydrophobic interactions with lipid tails, while for surfactants with short tails much fewer surfactants insert and then reversibly detach from the bilayer. This indicates the effect of the surfactant-tail length on the reversibility of the surfactant-bilayer interaction, in

agreement with experiments. Longer surfactants insert more deeply into the bilayer and increase the lateral dynamics of the bilayer, leading to the increased disorder of the bilayer, as observed in experimental observations that showed that longer ionic surfactants more significantly destabilize liposomes and supported monolayers. Simulations also show the insertion of fewer surfactants at 0.5 M NaCl than at 0 M because NaCl ions weaken the electrostatic interactions between imidazolium heads and lipid head groups.

These findings indicate that ionic surfactants have the electrostatic and hydrophobic interactions respectively with lipid heads and tails, both of which modulate their insertion and binding into the bilayer. Surfactants with shorter tails show the insertion of fewer surfactants, since their interactions with lipid bilayers depend on electrostatics rather than on hydrophobicity, leading to the reversible surfactant-bilayer interaction. In contrast, long surfactants have the strong hydrophobic interactions with lipid tails, and thus they more deeply insert and cannot be reversibly detached from the bilayer, yielding the increased dynamics of bilayers, which support the experimental observation of the dependence of membrane permeability and toxicity on the length of the ionic-surfactant tail.

### **Acknowledgments**

This research was supported by Basic Science Research Program through the National Research Foundation of Korea (NRF) funded by the Ministry of Education (NRF-2014R1A1A2054016).

## References

1. J. S. Wilkes, *Green Chemistry*, 2002, **4**, 73-80.
2. P. Wasserscheid, *Nature*, 2006, **439**, 797.
3. M. J. Earle, J. M. S. S. Esperança, M. A. Gilea, J. N. C. Lopes, L. P. N. Rebelo, J. W. Magee, K. R. Seddon and J. A. Widegren, *Nature*, 2006, **439**, 831-834.
4. T. Ueki and M. Watanabe, *Macromolecules*, 2008, **41**, 3739-3749.
5. H. Saruwatari, T. Kuboki, T. Kishi, S. Mikoshiba and N. Takami, *Journal of Power Sources*, 2010, **195**, 1495-1499.
6. T. Kuboki, T. Okuyama, T. Ohsaki and N. Takami, *Journal of Power Sources*, 2005, **146**, 766-769.
7. X. Han and D. W. Armstrong, *Accounts of Chemical Research*, 2007, **40**, 1079-1086.
8. M. Smiglak, A. Metlen and R. D. Rogers, *Accounts of Chemical Research*, 2007, **40**, 1182-1192.
9. Z. Conrad Zhang, in *Advances in Catalysis* 2006, vol. 49, pp. 153-237.
10. T. Welton, *Coordination Chemistry Reviews*, 2004, **248**, 2459-2477.
11. R. Rinaldi, R. Palkovits and F. Schüth, *Angewandte Chemie - International Edition*, 2008, **47**, 8047-8050.
12. N. V. Plechkova and K. R. Seddon, *Chemical Society Reviews*, 2008, **37**, 123-150.
13. Y. Pu, N. Jiang and A. J. Ragauskas, *Journal of Wood Chemistry and Technology*, 2007, **27**, 23-33.
14. A. Latała, P. Stepnowski, M. Nędzi and W. Mroziak, *Aquatic Toxicology*, 2005, **73**, 91-98.
15. R. J. Bernot, M. A. Brueseke, M. A. Evans-White and G. A. Lamberti, *Environmental Toxicology and Chemistry*, 2005, **24**, 87-92.

16. J. Pernak, K. Sobaszekiewicz and I. Mirska, *Green Chemistry*, 2003, **5**, 52-56.
17. C. Pretti, C. Chiappe, D. Pieraccini, M. Gregori, F. Abramo, G. Monni and L. Intorre, *Green Chemistry*, 2006, **8**, 238-240.
18. R. P. Swatloski, J. D. Holbrey and R. D. Rogers, *Green Chemistry*, 2003, **5**, 361-363.
19. M. Petkovic, K. R. Seddon, L. P. N. Rebelo and C. Silva Pereira, *Chemical Society Reviews*, 2011, **40**, 1383-1403.
20. K. O. Evans, *International Journal of Molecular Sciences*, 2008, **9**, 498-511.
21. K. O. Evans, *Journal of Physical Chemistry B*, 2008, **112**, 8558-8562.
22. K. O. Evans, *Colloids and Surfaces A: Physicochemical and Engineering Aspects*, 2006, **274**, 11-17.
23. S. Jeong, S. H. Ha, S. H. Han, M. C. Lim, S. M. Kim, Y. R. Kim, Y. M. Koo, J. S. So and T. J. Jeon, *Soft Matter*, 2012, **8**, 5501-5506.
24. M. Galluzzi, S. Zhang, S. Mohamadi, A. Vakurov, A. Podestà and A. Nelson, *Langmuir*, 2013, **29**, 6573-6581.
25. S. R. T. Cromie, M. G. Del Pópolo and P. Ballone, *Journal of Physical Chemistry B*, 2009, **113**, 11642-11648.
26. R. J. Bingham and P. Ballone, *Journal of Physical Chemistry B*, 2012, **116**, 11205-11216.
27. M. Klähn and M. Zacharias, *Physical Chemistry Chemical Physics*, 2013, **15**, 14427-14441.
28. D. Van Der Spoel, E. Lindahl, B. Hess, G. Groenhof, A. E. Mark and H. J. C. Berendsen, *Journal of Computational Chemistry*, 2005, **26**, 1701-1718.
29. E. Lindahl, B. Hess and D. van der Spoel, *Journal of Molecular Modeling*, 2001, **7**, 306-317.

30. B. Hess, C. Kutzner, D. van der Spoel and E. Lindahl, *Journal of Chemical Theory and Computation*, 2008, **4**, 435-447.
31. G. A. Kaminski, R. A. Friesner, J. Tirado-Rives and W. L. Jorgensen, *Journal of Physical Chemistry B*, 2001, **105**, 6474-6487.
32. W. L. Jorgensen, D. S. Maxwell and J. Tirado-Rives, *Journal of the American Chemical Society*, 1996, **118**, 11225-11236.
33. D. P. Tieleman, J. L. MacCallum, W. L. Ash, C. Kandt, Z. Xu and L. Monticelli, *Journal of Physics Condensed Matter*, 2006, **18**, S1221-S1234.
34. E. Han and H. Lee, *Physical Chemistry Chemical Physics*, 2014, **16**, 981-988.
35. S. V. Sambasivarao and O. Acevedo, *Journal of Chemical Theory and Computation*, 2009, **5**, 1038-1050.
36. J. Mondal, E. Choi and A. Yethiraj, *Macromolecules*, 2014, **47**, 438-446.
37. T. Méndez-Morales, J. Carrete, M. Pérez-Rodríguez, Ó. Cabeza, L. J. Gallego, R. M. Lynden-Bell and L. M. Varela, *Physical Chemistry Chemical Physics*, 2014, **16**, 13271-13278.
38. B. Docampo-Álvarez, V. Gómez-González, T. Méndez-Morales, J. Carrete, J. R. Rodríguez, Ó. Cabeza, L. J. Gallego and L. M. Varela, *Journal of Chemical Physics*, 2014, **140**.
39. T. Méndez-Morales, J. Carrete, S. Bouzón-Capelo, M. Pérez-Rodríguez, O. Cabeza, L. J. Gallego and L. M. Varela, *Journal of Physical Chemistry B*, 2013, **117**, 3207-3220.
40. J. Carrete, T. Méndez-Morales, M. García, J. Vila, O. Cabeza, L. J. Gallego and L. M. Varela, *Journal of Physical Chemistry C*, 2012, **116**, 1265-1273.
41. U. Essmann, L. Perera, M. L. Berkowitz, T. Darden, H. Lee and L. G. Pedersen, *Journal*

- of Chemical Physics*, 1995, **103**, 8577-8593.
42. G. Bussi, D. Donadio and M. Parrinello, *Journal of Chemical Physics*, 2007, **126**.
43. H. J. C. Berendsen, J. P. M. Postma, W. F. van Gunsteren, A. DiNola and J. R. Haak, *Journal of Chemical Physics*, 1984, **81**, 3684-3690.
44. B. Hess, *Journal of Chemical Theory and Computation*, 2008, **4**, 116-122.
45. R. A. Böckmann, A. Hac, T. Heimburg and H. Grubmüller, *Biophysical Journal*, 2003, **85**, 1647-1655.
46. I. C. Yeh and G. Hummer, *Journal of Physical Chemistry B*, 2004, **108**, 15873-15879.
47. A. Filippov, G. Orädd and G. Lindblom, *Biophysical Journal*, 2003, **84**, 3079-3086.
48. M. Kim, H. R. Kim, S. Y. Chae, R. G. Larson, H. Lee and J. C. Park, *Journal of Physical Chemistry B*, 2013, **117**, 6917-6926.
49. S. Y. Woo and H. Lee, *Langmuir*, 2014, **30**, 8848-8855.
50. E. Han and H. Lee, *RSC Advances*, 2015, **5**, 2047-2055.
51. W. Humphrey, A. Dalke and K. Schulten, *Journal of Molecular Graphics*, 1996, **14**, 33-38.

Table 1. List of simulations.

Surfactant type	Name	No. of surfactants	No. of ions		No. of surfactants inserted into the bilayer at 250 ns
			Na <sup>+</sup> Cl <sup>-</sup>	counterions (Cl <sup>-</sup> )	
C <sub>2</sub> MIM	C <sub>2</sub> M16	16	-	16	5
	C <sub>2</sub> M16i	16	79	16	2
	C <sub>2</sub> M60	60	-	60	10
C <sub>4</sub> MIM	C <sub>4</sub> M16	16	-	16	15
	C <sub>4</sub> M16i	16	79	16	6
	C <sub>4</sub> M60	60	-	60	27
C <sub>6</sub> MIM	C <sub>6</sub> M16	16	-	16	15
	C <sub>6</sub> M16i	16	79	16	12
	C <sub>6</sub> M60	60	-	60	40
C <sub>10</sub> MIM	C <sub>10</sub> M16	16	-	16	15
	C <sub>10</sub> M16i	16	79	16	6
	C <sub>10</sub> M60	60	-	60	13

Figure 1. Snapshots of the cross section of the ionic surfactant-bilayer system at the beginning (0 ns; left) and end of simulations (250 ns; columns 2-7). Initial configuration is shown only for  $C_{10}M16$ , but this random configuration is applied for all other systems. Black, brown, and light-blue colors respectively represent ionic surfactants, DOPC phosphates and hydrocarbon tails. For NaCl ions,  $Na^+$  and  $Cl^-$  ions are colored in blue and red. The explicit water and counterions ( $Cl^-$ ) are omitted for clarity. The images were created with Visual Molecular Dynamics.<sup>51</sup>

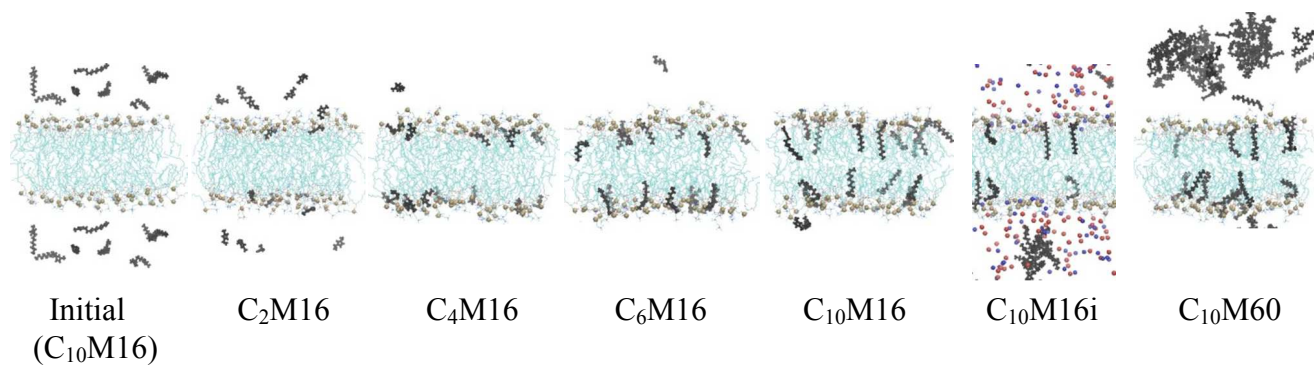


Figure 2. Number of ionic surfactants inserted into lipid bilayers as a function of time.

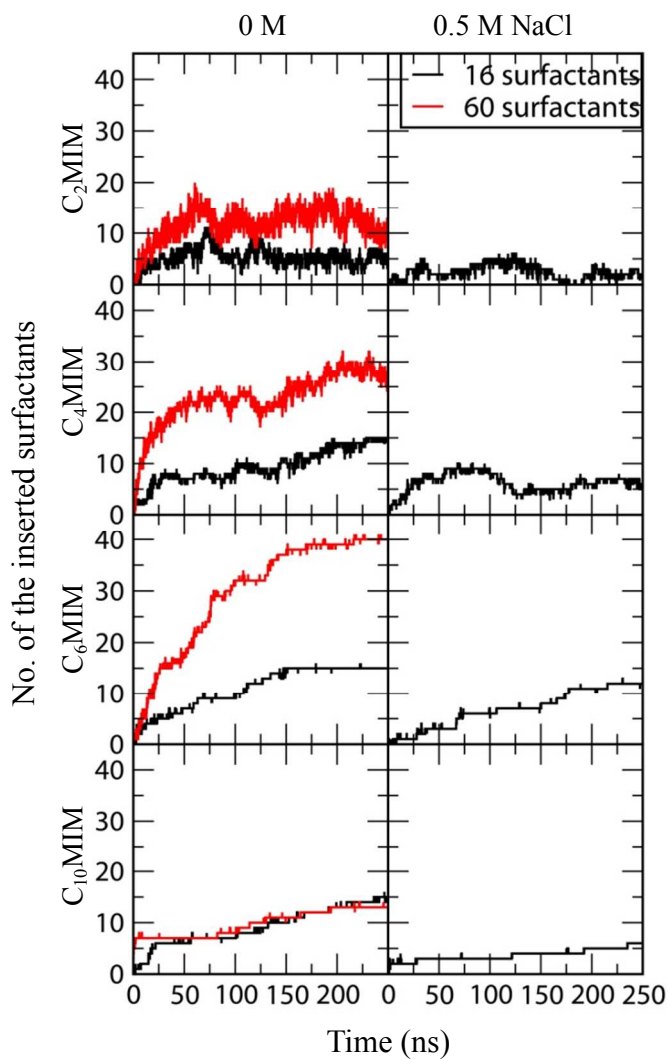


Figure 3. Average number of carbon atoms of DOPC tails close to each surfactant as a function of time (top), and cumulative number of carbon atoms of DOPC tails as a function of distance from the surfactant tail (bottom).

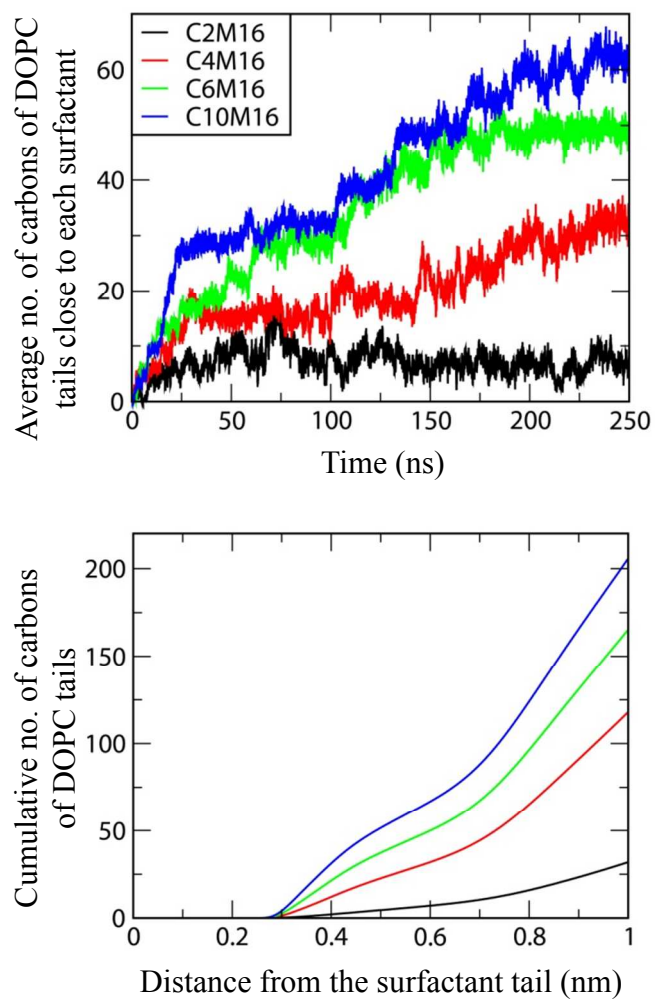


Figure 4. Mass density profiles of ionic surfactants, DOPC lipids, and NaCl ions.

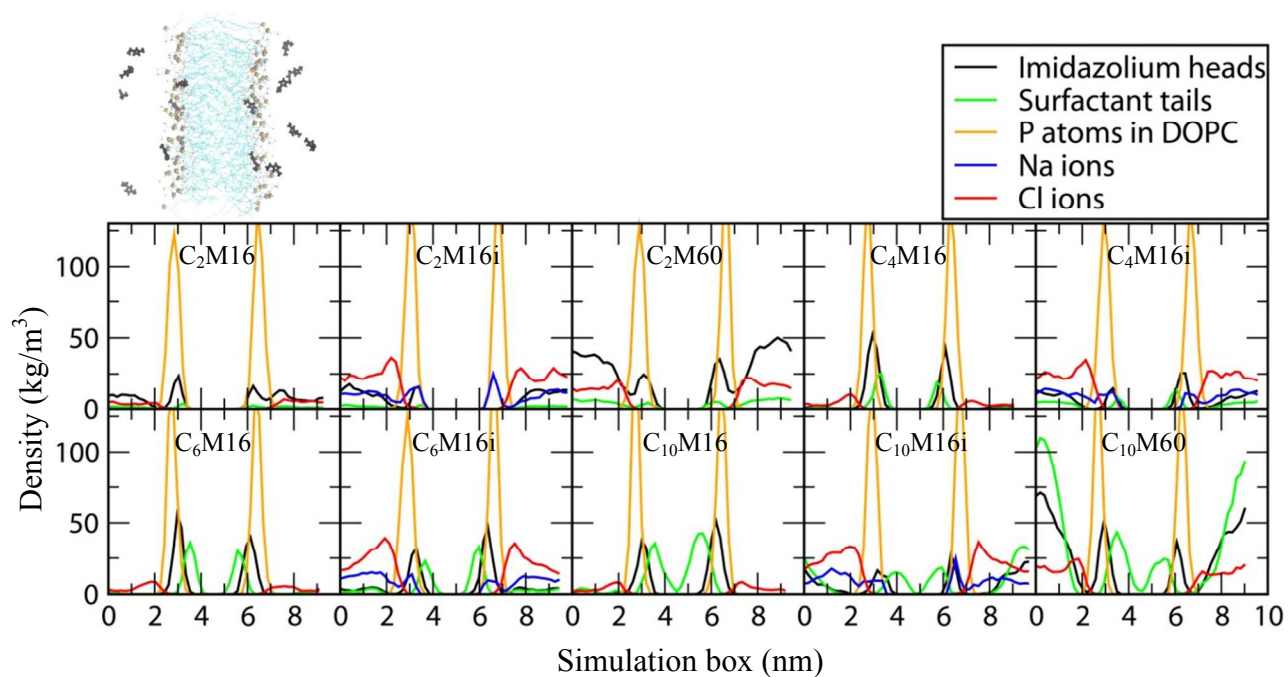


Figure 5. Radial distribution functions between DOPC phosphorus atoms and Na ions

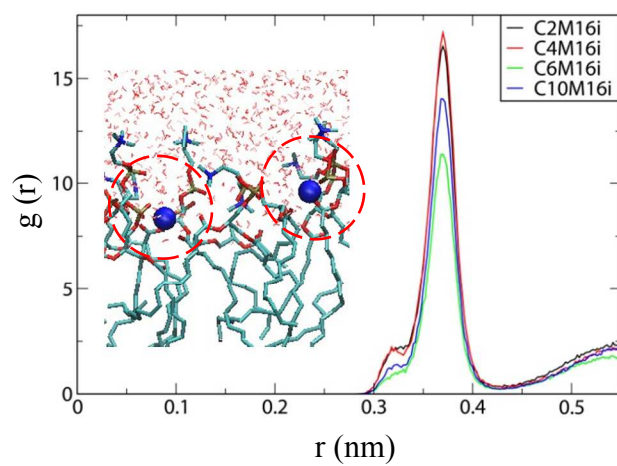


Figure 6. Coordinates of the terminal carbon of each surfactant's tail in the bilayer normal direction (z-direction) as a function of time. Dotted red lines represent the average position of P atoms of DOPC lipids, and solid lines with 16 different colors designate the position for the terminal carbon of each surfactant tail. To analyze complete trajectories, periodic images are considered in z-direction.

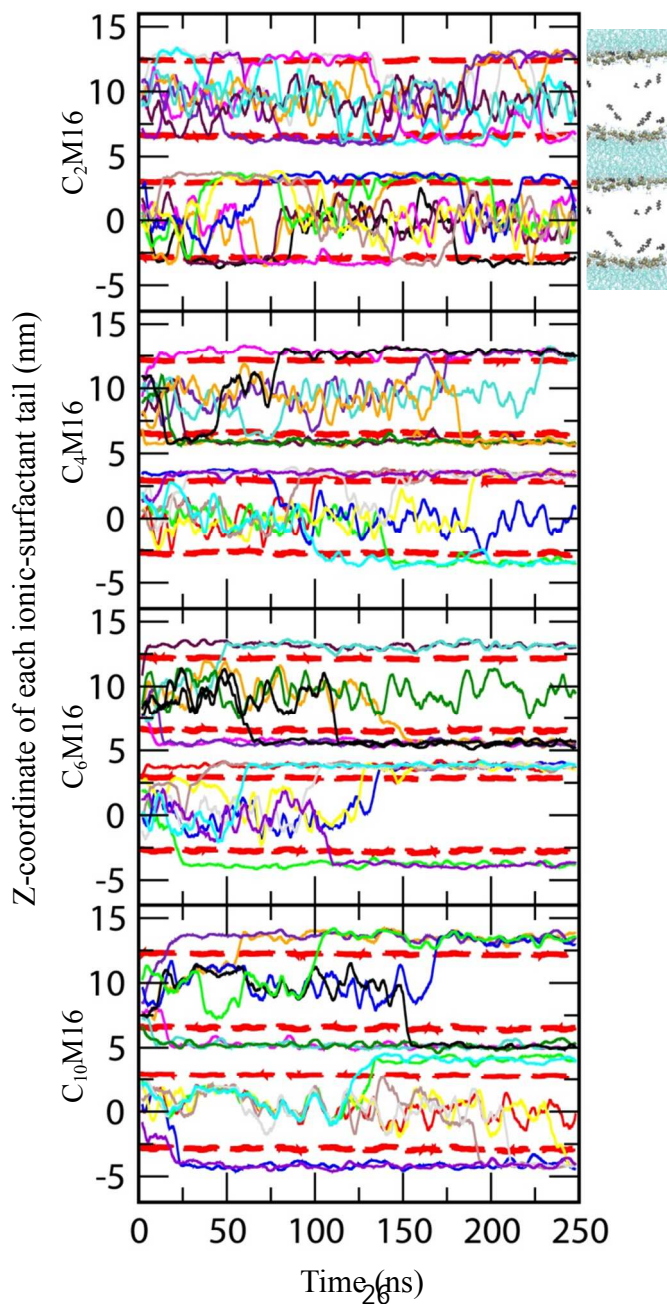


Figure 7. The number of ionic surfactants inserted into lipid bilayers (square) and lateral diffusion coefficients of DOPC lipids ( $D$ ; circle) for the systems with 16 ionic surfactants ( $C_nM16$ ), as a function of the number of hydrocarbons in the surfactant tail ( $n$ ). The lateral diffusivity of pure DOPC bilayer is shown in  $n = 0$ .

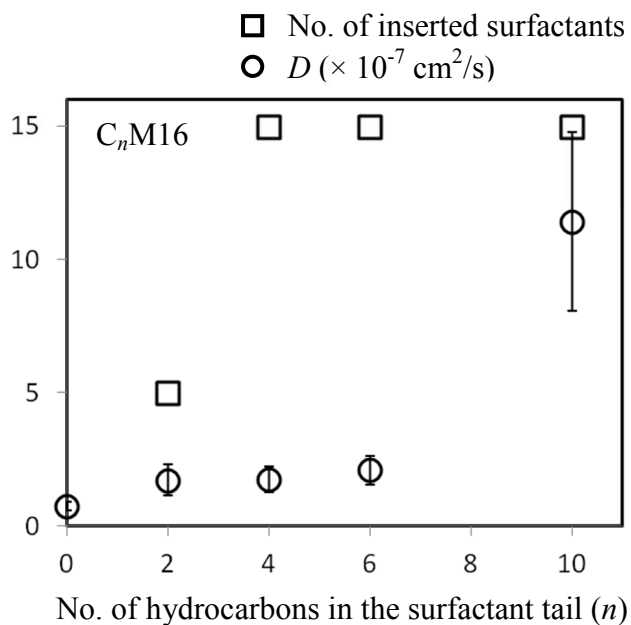


Figure 8. Number of ionic-surfactant molecules in the largest cluster as a function of the number of carbons in the surfactant tail.

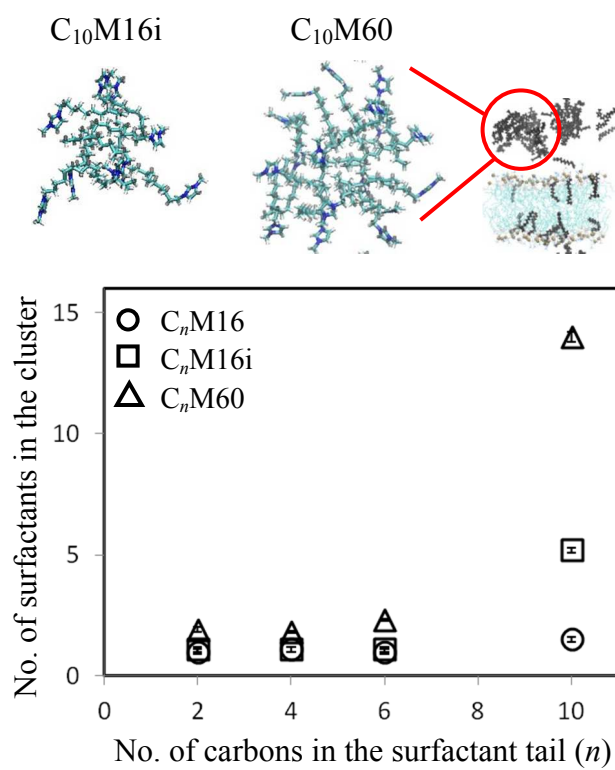


Figure 9. Snapshots of the ionic-surfactant insertion into the lipid bilayer. Either a head or a tail of the surfactant binds to the bilayer surface (respectively, top and bottom images). The imidazolium headgroup is highlighted in red circles.

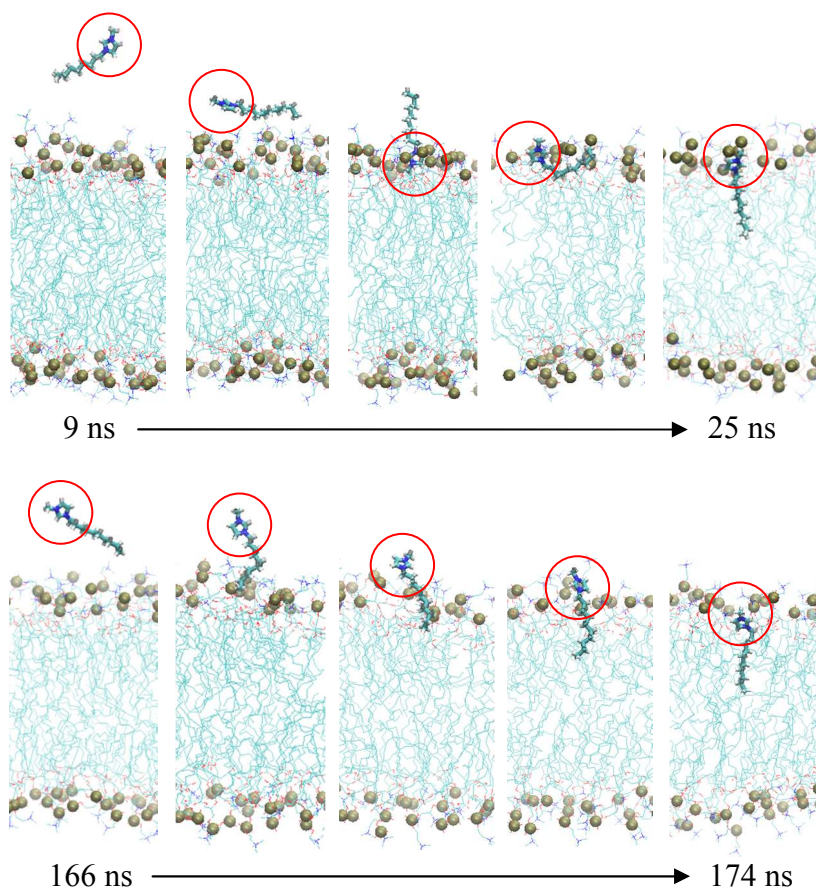
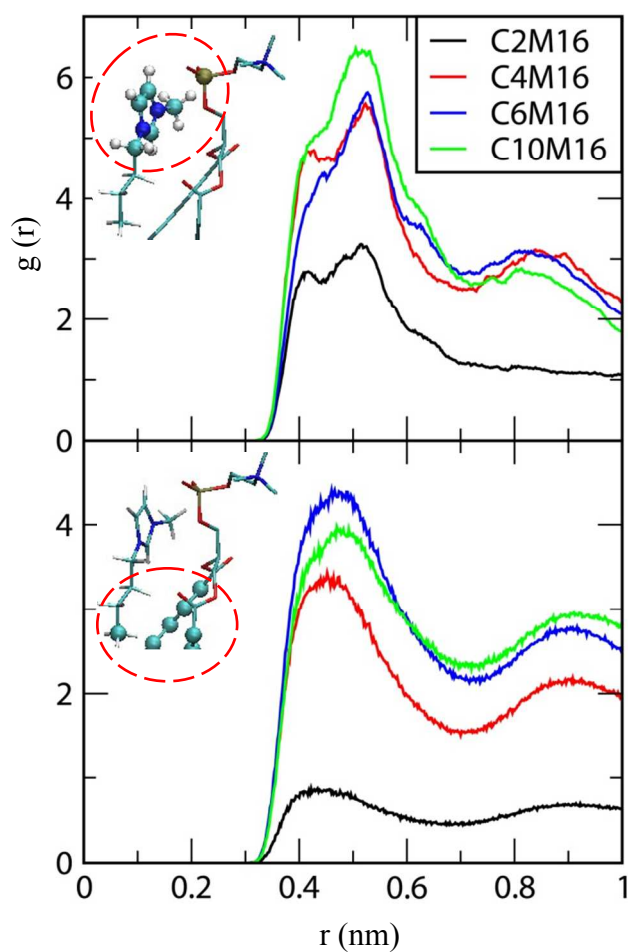


Figure 10. Radial distribution functions between the DOPC phosphorus atom and the center of mass of the surfactant headgroup (top), and between the DOPC tail and the terminal carbon of surfactant (bottom).



For Table of Contents use only

Title: The Binding and Insertion of Imidazolium-based Ionic Surfactants into Lipid Bilayers: the Effects of Surfactant Size and Salt Concentration

Author: Hwankyu Lee, Tae-Joon Jeon

